

Charm Decays and Spectroscopy at BABAR

Romulus Godang*[†]

On Behalf of the BABAR Collaboration

Department of Physics

University of South Alabama

ILB 115, 307 University Blvd., N.

E-mail: godang@usouthal.edu

SLAC-PUB-15329

We present searches for rare charm decays of the form $X_c^+ \rightarrow h^\pm \ell^\mp \ell^{(\prime)\pm}$, where X_c^+ is a charm hadron either D^+ , D_s^+ , or Λ_c^+ , and $\ell^{(\prime)\pm}$ is an electron or muon. These modes are based on 384 fb^{-1} of e^+e^- annihilation data collected at the $\Upsilon(4S)$ resonance with the BABAR detector at the SLAC National Accelerator Laboratory. We also present the flavor-changing neutral-current decays $D^0 \rightarrow e^+e^-$, $D^0 \rightarrow \mu^+\mu^-$, and $D^0 \rightarrow e^\pm\mu^\mp$ that corresponds to an integrated luminosity of 468 fb^{-1} of data. The decay $D^0 \rightarrow e^+\mu^-$ is further lepton-flavor violating, and thus occur only through very slow neutrino mixing. These decays constitute sensitive probes for possible new-physics contribution. We report new limits on the branching fractions of these decays.

36th International Conference on High Energy Physics,

July 4-11, 2012

Melbourne, Australia

*Speaker.

[†]This work was supported by the U.S. Department of Energy under grant No. DE-FG02-96ER-40970

1. INTRODUCTION

In the Standard Model (SM), the flavor-changing neutral processes are very rare and are of obvious interest in the search for new physics. In the Flavor-Changing Neutral Current (FCNC) decays $D^0 \rightarrow \ell^+ \ell^-$, where ℓ is an either electron or muon, are strongly suppressed by the Glashow-Iliopoulos-Maiani (GIM) mechanism [1]. These decays cannot occur at tree level in the SM. The branching fraction of the decays $D^0 \rightarrow \ell^+ \ell^-$ are predicted to be $\mathcal{O}(10^{-13})$ [2].

Most of the attention on FCNC decays has been focused in the K and B meson sectors and less in the charm meson sector. It is due to the fact that the SM expectations for $D^0 - \bar{D}^0$ mixing are very small compared to the $K^0 - \bar{K}^0$ and $B^0 - \bar{B}^0$ mixing. However, the FCNC decay in the charm sector is unique due to its decays involve an up-type quark which implies into an effective GIM cancellations and new physics. The decay modes of Lepton-Flavor Violating (LFV) which corresponding to two leptons with two oppositely charged of different flavor and Lepton-Number Violating (LNV) decays where two leptons have the same charge are forbidden in the SM.

Figure 1 shows the Standard Model short-distance contributions to the $c \rightarrow u \ell^+ \ell^-$ transition. The branching fraction for the decay of $D \rightarrow X_u \ell^+ \ell^-$ is predicted to be $\mathcal{O}(10^{-8})$ [2, 3]. The decay of $c \rightarrow u \ell^+ \ell^-$ is screened by the long distance contributions. It is also expected to dominate over the short distance contributions in $D^0 - \bar{D}^0$ mixing. The long distance contributions were shown to be largely dominant in $c \rightarrow u \ell^+ \ell^-$. The experimental upper bounds on the branching fraction of $c \rightarrow u \ell^+ \ell^-$ is presently in the range of $\mathcal{O}(10^{-5})$ [4]. It is an order of magnitude larger than the Standard Model prediction for specific channels [5]. The highest rate of $D \rightarrow V \ell^+ \ell^-$ channel with $V = \rho, \omega, \phi, K^*$ is the decay of $D_s^+ \rightarrow \rho^+ \ell^+ \ell^-$. It is predicted at the highest rate $\approx 3 \times 10^{-5}$, however there are unfortunately no experimental data on this channel.

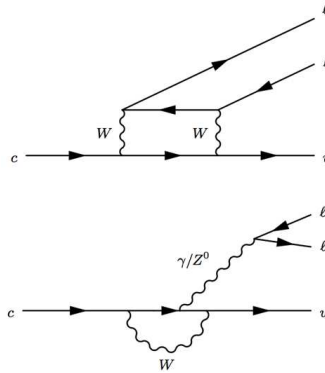


Figure 1: Standard Model short-distance contributions to the $c \rightarrow u \ell^+ \ell^-$ transition.

2. The BABAR DETECTOR AND DATA SET

The BABAR detector was operated at the PEP-II asymmetric-energy storage rings at the SLAC National Accelerator Laboratory. The data used in this analysis were collected with the BABAR detector. The data sample consist of an integrated luminosity of 384 fb^{-1} for $X_c^+ \rightarrow h^\pm \ell^\mp \ell^{(\prime)+}$ and 468 fb^{-1} for $D^0 \rightarrow \ell^+ \ell^-$ accumulated at the $\Upsilon(4S)$ resonance and 40 MeV below the $\Upsilon(4S)$

resonance. The asymmetric energy of the PEP-II e^+ and e^- beams result in a Lorentz boost $\beta\gamma \approx 0.55$ of the $B\bar{B}$ pairs.

A detail description of the BABAR detector is presented elsewhere [6]. The momenta of the charged particles are measured in a tracking system consisting of a 5-layer double sided silicon vertex tracker (SVT) and a 40-layer drift chamber (DCH). The SVT and DCH operate within a 1.5 T solenoid field and have a combined solid angle coverage in the center of mass frame of 90.5%. A detector of internally reflected Cerenkov radiation (DIRC) is used for charged particle identifications of pions, kaons, and protons with likelihood ratios calculated from dE/dx measurements in the SVT and DCH. Photons and long-lived neutral hadrons are detected and their energies are measured in a CsI(Tl) electromagnetic calorimeter (EMC). For electrons, energy lost due to bremsstrahlung is recovered from deposits in the EMC.

3. ANALYSIS

We select charm hadron candidates X_c with center of mass frame momentum greater than 2.5 GeV/c to suppress combinatoric background. The e^+e^- invariant mass is required to be greater than 200 MeV/ c^2 in order to reject photon conversion and π^0 decays to $e^+e^-\gamma$. For the $D_{(s)}^+ \rightarrow \pi\phi$, $\phi \rightarrow \ell^+\ell^-$ decay mode, we excluded events with $0.95 < m(e^+e^-) < 1.05$ GeV/ c^2 and $0.99 < m(\mu^+\mu^-) < 1.05$ GeV/ c^2 to reject the decays through the ϕ resonance. The QED backgrounds was suppressed by requiring at least five tracks in the event and that hadron candidate be consistent with the electron hypothesis. After the initial event selection, significant combinatorial background contribution, we use three discriminating variables in likelihood ratio: charm hadron candidate, total reconstructed energy in the event, and flight length significance.

To measure the signal events we use extended, unbinned, maximum-likelihood. These signals are converted to the known charm branching fractions by normalization. To reduce the systematic effects we choose normalization modes with kinematics similar to the kinematic of the signal decays. For decays of D^+ and D_s^+ mesons, the normalization mode is $\pi^+\phi$ where $\phi \rightarrow K^+K^-$. For the decays of Λ_c^+ , we choose the decays of $\Lambda_c^+ \rightarrow pK^-\pi^+$. Figures 2–6 show the fitting results of the invariant mass of $X_c^+ \rightarrow h^\pm \ell^\mp \ell^{(\prime)+}$ decays. The dashed curves show the background components for the dimuon modes in which muon candidates arise from misidentified hadrons. Detail information on the likelihood selection, fitting procedure, systematic uncertainties, and fit results are available here [7]. We calculate the upper limits on the ratio of the branching fractions at 90% confidence level (CL): $\mathcal{B}(D_{(s)}^+ \rightarrow \pi^\pm \ell^\mp \ell^{(\prime)+})/\mathcal{B}(D_{(s)}^+ \rightarrow \pi^+\phi)$, $\mathcal{B}(D_{(s)}^+ \rightarrow K^\pm \ell^\mp \ell^{(\prime)+})/\mathcal{B}(D_{(s)}^+ \rightarrow \pi^+\phi)$, and $\mathcal{B}(\Lambda_c^+ \rightarrow p^{(-)} \ell^\mp \ell^{(\prime)+})/\mathcal{B}(\Lambda_c^+ \rightarrow pK^-\pi^+)$. The most significant signal is seen in the decay of $\Lambda_c^+ \rightarrow p\mu^+\mu^-$ with yield of $11.1 \pm 5.0(stat) \pm 2.5(syst)$. It has a statistical significant of 2.6σ . It is corresponding to 90% CL upper limit on the branching fraction of 44×10^{-6} .

We also recently measured the flavor-changing neutral-current decays $D^0 \rightarrow e^+e^-$, $D^0 \rightarrow \mu^+\mu^-$, and $D^0 \rightarrow e^\pm\mu^\mp$ that corresponds to an integrated luminosity of 468 fb $^{-1}$ of data. To normalize the decays of $D^0 \rightarrow \ell^+\ell^-$, we use $D^0 \rightarrow \pi^+\pi^-$ control sample and applying a linear combination of Fisher discriminant [8] of the following five variables: measured D^0 flight length, $|\cos\theta_{hel}|$ angle between the momentum of the positively-charged D^0 daughter and the boost direction from the lab frame to the D^0 rest frame (all in the D^0 rest frame), the missing transverse momentum with respect to the beam axis, the ratio of the 2nd and 0th Fox-Wolfram moments [9],

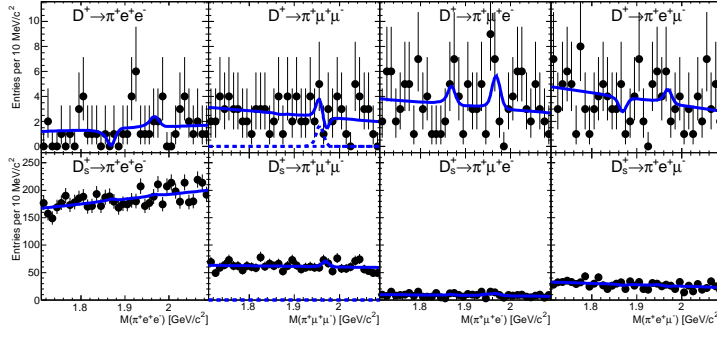


Figure 2: Invariant-mass distributions for $D^+ \rightarrow \pi^+ \ell^+ \ell'^{-}$ (top) and $D_s^+ \rightarrow \pi^+ \ell^+ \ell'^{-}$ (bottom) candidates. The fit results shown in the solid line.

and the D^0 momentum in the center of mass frame. To remove the continuum combinatoric background we use the $|\cos\theta_{\text{hel}}|$ variable. Figure 7 shows distributions of $|\cos\theta_{\text{hel}}|$ before applying a minimum Fisher discriminant.

The branching fraction of $D^0 \rightarrow \ell^+ \ell^-$ is given by the following expressions:

$$\mathcal{B}_{\ell\ell} = \left(\frac{N_{\ell\ell}}{N_{\pi\pi}^{\text{fit}}} \right) \left(\frac{\epsilon_{\pi\pi}}{\epsilon_{\ell\ell}} \right) \mathcal{B}_{\pi\pi} = S_{\ell\ell} \cdot N_{\ell\ell} \quad (3.1)$$

where $S_{\ell\ell}$ is defined by

$$S_{\ell\ell} \equiv \frac{\mathcal{B}_{\pi\pi}}{N_{\pi\pi}^{\text{fit}}} \frac{\epsilon_{\pi\pi}}{\epsilon_{\ell\ell}}. \quad (3.2)$$

and N_{obs} is defined by

$$N_{\text{obs}} = \mathcal{B}_{\ell\ell}/S_{\ell\ell} + N_{BG}. \quad (3.3)$$

The $N_{\ell\ell}$ and $N_{\pi\pi}^{\text{fit}}$ are the number of $D^0 \rightarrow \ell^+ \ell^-$ and $D^0 \rightarrow \pi^+ \pi^-$ candidates, respectively. The $\mathcal{B}_{\pi\pi} = (1.400 \pm 0.026) \times 10^{-3}$ [10]. We use the likelihood ratio ordering principle of Feldman and Cousins [11] to determine 90% CL intervals. We find one event of $D^0 \rightarrow e^+ e^-$ with background of 1.0 ± 0.5 events and two events of $D^0 \rightarrow e^\pm \mu^\mp$ with background of 1.4 ± 0.3 events. These correspond to the 90% CL upper limits for the branching fractions $< 1.7 \times 10^{-7}$ for $D^0 \rightarrow e^+ e^-$ and $< 3.3 \times 10^{-7}$ for $D^0 \rightarrow e^\pm \mu^\mp$. For the $D^0 \rightarrow \mu^+ \mu^-$ channel, we find eight events with expected background of 3.9 ± 0.6 . This corresponds to 90% CL upper limits on the branching fraction of $[0.6, 8.1] \times 10^{-7}$. Detail information on the likelihood selection, fitting procedure, systematic uncertainties, and fit results are available here [12].

4. CONCLUSIONS

We have searched for the decay modes $D_{(s)}^+ \rightarrow \pi^\pm \ell^\mp \ell'^{(\prime)+}$, $D_{(s)}^+ \rightarrow K^\pm \ell^\mp \ell'^{(\prime)+}$, and $\Lambda_c^+ \rightarrow p^{(-)} \ell^\mp \ell'^{(\prime)+}$. No signals are observed and we report upper limits on 35 different branching ratios between 0.4×10^{-4} and 37×10^{-4} at 90% CL. This corresponds to limits on the branching fractions between 1×10^{-6} and 44×10^{-6} .

We also have searched for the leptonic charm decays $D^0 \rightarrow e^+ e^-$, $D^0 \rightarrow \mu^+ \mu^-$, and $D^0 \rightarrow e^\pm \mu^\mp$. We find no statistically significant excess over the expected background. These results supersede our previous results [13] and are consistent with the results of the Belle experiment [14].

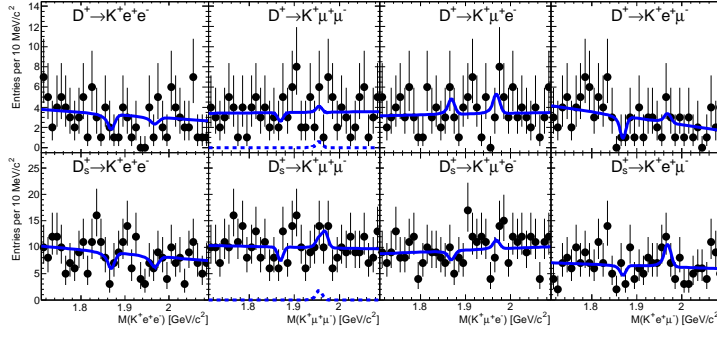


Figure 3: Invariant-mass distributions for $D^+ \rightarrow K^+ \ell^+ \ell^{(\prime)-}$ (top) and $D_s^+ \rightarrow K^+ \ell^+ \ell^{(\prime)-}$ (bottom) candidates. The fit results shown in the solid line.

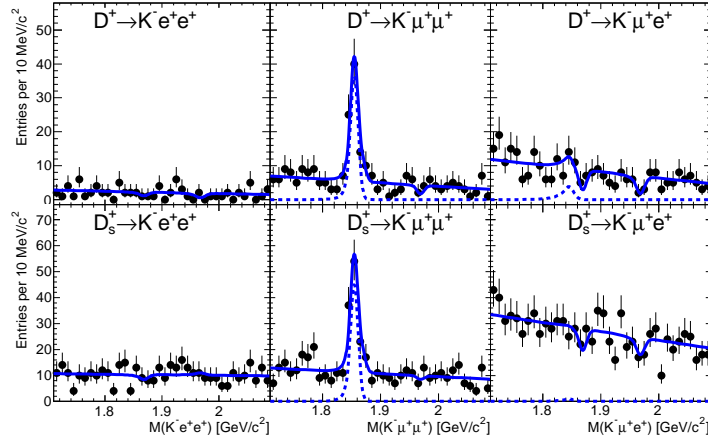


Figure 4: Invariant-mass distributions for $D^+ \rightarrow K^- \ell^+ \ell^{(\prime)+}$ (top) and $D_s^+ \rightarrow K^- \ell^+ \ell^{(\prime)+}$ (bottom) candidates. The fit results shown in the solid line.

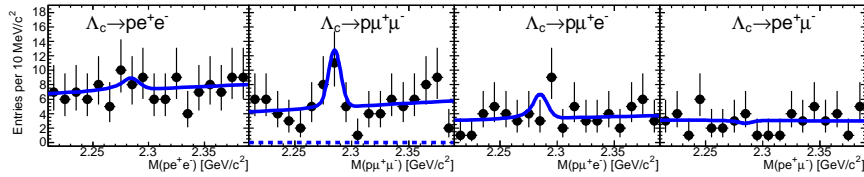


Figure 5: Invariant-mass distributions for $\Lambda_c^+ \rightarrow p \ell^+ \ell^{(\prime)-}$ candidates. The fit results shown in the solid line.

5. ACKNOWLEDGMENTS

The author would like to thank the organizers of ICHEP 2012, the 36th International Conference on High Energy Physics, Melbourne, Australia. The supports from the BABAR Collaboration, the University of South Alabama, and the University of Mississippi are gratefully acknowledged.

References

- [1] S. L. Glashow, J. Iliopoulos, and L. Maiani, Phys. Rev. D **2**, 1285, (1970).

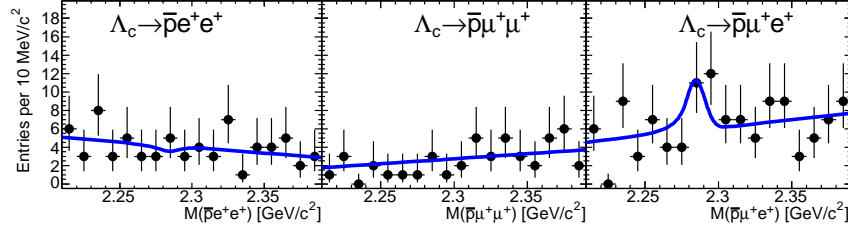


Figure 6: Invariant-mass distributions for $\Lambda_c^+ \rightarrow \bar{p}\ell^+\ell^{(\prime)+}$ candidates. The fit results shown in the solid line.

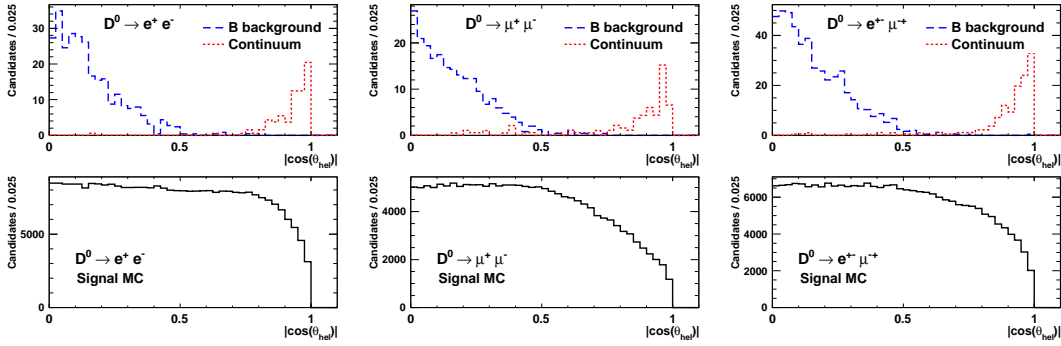


Figure 7: Distributions of $|\cos(\theta_{\text{hel}})|$ for the three signal channels: $D^0 \rightarrow e^+e^-$ (left), $D^0 \rightarrow \mu^+\mu^-$ (center), and $D^0 \rightarrow e^\pm\mu^\mp$ (right). The bottom distributions show the signal Monte Carlo samples with an arbitrary normalization.

- [2] G. Burdman, E. Golowich, J. Hewett, and S. Pakwasa, Phys. Rev. D **66**, 014009, (2002).
- [3] S. Fajfer, S. Prelovsek, and P. Singer, Phys. Rev. D **64**, 114009, (2001).
- [4] E791 Collaboration, E. M. Aitala *et al.*, Phys. Rev. Lett. **86**, 3969 (2001).
- [5] S. Fajfer, S. Prelovsek, and P. Singer, Phys. Rev. D **58**, 094038, (1998).
- [6] BABAR Collaboration, B. Aubert *et al.*, Nucl. Instr. Methods Phys. Res., Sect. A **479**, 1 (2002).
- [7] BABAR Collaboration, J. P. Lees *et al.*, Phys. Rev. D **84**, 072006 (2011).
- [8] R. A. Fisher, Annals of Eugenics **7**, 179 (1936).
- [9] G.C. Fox and S. Wolfram, Phys. Rev. Lett. **41**, 1581 (1978).
- [10] Particle Data Group, K. Nakamura *et al.*, Journal of Phys. G **37**, 075021 (2010).
- [11] G.J. Feldman and R.D. Cousins, Phys. Rev. D **57**, 3873 (1998).
- [12] BABAR Collaboration, J. P. Lees *et al.*, Phys. Rev. D **86**, 032001 (2012).
- [13] BABAR Collaboration, B. Aubert *et al.*, Phys. Rev. Lett. **93**, 191801 (2004).
- [14] Belle Collaboration, M. Petric *et al.*, Phys. Rev. D **81**, 091102(R) (2010).